Abstract

Simulating the mechanical behaviour of heterogeneous structures often requires building an equivalent homogeneous finite element model in order to reduce the number of degrees of freedom. Indeed, modelling complex structures, analysing their dynamic behaviours and updating the models with experimental data all need approximating global properties with equivalent homogeneous materials. This is a reason why so-called "homogenization" techniques have been developed, to recreate a given structure's behaviour by reducing the multiplicity of its components' properties and by enabling the control of the entire model's properties. Such methods are much desired for modelling composite materials and complex structures such as laminated stators of electric machines. While very accurate analytical results have been found in the field of 2D-dynamics of composite structures, relatively few mature methods yet exist for the identification of equivalent materials, independent from the structure's dimensions and applicable to finite element modelling. For 3D-homogenization and in particular for heterogeneous structures in which no simplifying assumptions can be made, there remains much to develop.

In this paper, a novel method of equivalent material identification is proposed for orthotropic and multi-layered laminated structures. It gathers a set of simple static simulations on finite element models (i.e. virtual testing), inspired from experimental testing processes, in order to identify the equivalent material's nine elastic coefficients directly: Young's moduli, shear moduli and Poisson's coefficients. Unlike the other homogenization techniques, the method may be applied to superelements in addition to fully-defined finite element models. The method is applied to the models of two stators of electric cars. As it is usually the case, a stator consists of a stack of several hundreds of steel sheets, less than a half-millimetre-thick and separated from each other by an insulating resin in order to prevent eddy currents from taking place. Taking into account the additional heterogeneity due to the weld beads in the stator's lateral face, the model is divided into several zones, each of which stands for a specific equivalent material. The simulations performed in low frequencies enable predicting both real stators' dynamic behaviours with good precision, according to experimental data. In particular, the cylinder modes, most critical for industrial studies due to their high probability of coincidence with electromagnetic excitations, are well predicted. These results offer interesting perspectives in the prediction of the dynamic behaviours of stators of electric machines during design stages, without need of time-consuming and delicate model updating procedures with experimental data from expensive prototypes.

Keywords: homogenization, laminated structures, equivalent homogeneous material, stator of electric machine, superelements

1 Introduction

Modelling a complex structure's individual components may become difficult if they are numerous, small, or if some of the assembly properties are not known. This is why so-called "homogenization" methods have been developed, to reduce the number of degrees of freedom in a given heterogeneous structure. Such methods are often used for modelling composite materials, and especially for laminated structures. A short review of some existing homogenization techniques is given, as well as brief discussions over their uses.

Concerning stratified materials, the assumption of plane stresses and strains tends to simplify many applications (for instance with laminated beams or shells), for which the theory predicts static and dynamic behaviours with good accuracy (cf. [1, 2]). Some other analyses however can not be simplified by such assumptions (for example if no dimension can be neglected in the model), and have to be meshed in 3D.

First of all, the relations that may be the simplest for determining a homogeneous equivalent material to a 3D-laminated structure, and that are used in the reference works in the field of composite materials, such as [2] and [3], are weighted averages of the different components' elastic constants, sometimes referred to as the "rule of mixtures". The expressions are based on the direct identification of an equivalent material's elastic constants, have relatively low resource demands, and already give a good approximation of the structure's global behaviour. However, their applicability is limited to stacks of isotropic layers. The analytical method developed by Begis et al. [4] aims at determining any structure's equivalent elasticity matrix from its components' elasticity matrices, that may even describe a triclinic behaviour, the most general material definition without any symmetries or simplifications. The general relation used to describe a material's stress-strain behaviour is Hooke's law $\{\sigma\} = C\{\varepsilon\}$, where $\{\sigma\}$ is the stress tensor, C the elasticity matrix and $\{\varepsilon\}$ the strain tensor [5]. The entire linear system is defined as following:

$$\begin{Bmatrix} \sigma_{11} \\ \sigma_{22} \\ \sigma_{33} \\ \\ \sigma_{23} \\ \sigma_{13} \\ \sigma_{12} \end{Bmatrix} = \begin{bmatrix} c_{11} & c_{12} & c_{13} & c_{14} & c_{15} & c_{16} \\ & c_{22} & c_{23} & c_{24} & c_{25} & c_{26} \\ & & c_{33} & c_{34} & c_{35} & c_{36} \\ \\ & & & c_{44} & c_{45} & c_{46} \\ & \text{sym.} & & & c_{55} & c_{56} \\ & & & & & c_{66} \end{bmatrix} \begin{Bmatrix} \varepsilon_{11} \\ \varepsilon_{22} \\ \varepsilon_{33} \\ \\ 2 \cdot \varepsilon_{23} \\ 2 \cdot \varepsilon_{13} \\ 2 \cdot \varepsilon_{12} \end{Bmatrix}, \qquad (1)$$

where the indices 1, 2 and 3 respectively refer to the directions x, y and z.

Tackling the same issues, this method was compared in [6] to the works [7] and [8], and has been declared more accurate by the authors. Amongst others, the articles of Lukkassen et al. [9], Chung et al. [10], Hassan et al. [11] and Kalamkarov et al. [12] were based on the same general expressions and have proposed similar analytic approaches, but remain difficult to establish by lack of detailed applications.

At the opposite from analytical and numerical methods, many studies have been focused on the experimental determination of a given structure's elastic behaviour. Amongst others, several ways to calculate a structure's entire elasticity matrix (that may even be triclinic) were detailed by Hearmon [13] and Hayes [14], needing however several types of samples, and very difficult to apply to finite element models. Yet because of this same difficulty, the uses of other methods such as those developed in the articles of Pierron et al. [15], Rikards et al. [16, 17, 18] and Araújo et al. [19] were also compromised.

The following sections will present the development of a new method for the identification of elastic properties applied to multi-layered orthotropic laminates. In addition to this, application examples on heterogeneous FE models and the comparison with experimental results for the stator of an electric motor will be shown.

2 Identification method for multi-layered orthotropic laminates

In this section, a new approach for determining a heterogeneous structure's elastic properties is proposed. The equivalent material defined is orthotropic and is characterised by nine elastic coefficients: E_x, E_y, E_z, G_{zy}, G_{zx}, G_{xy}, ν_{yz}, ν_{xz} and ν_{xy}. The method has been initially inspired from experimental analyses described in [2]. The structure taken as an example in this section is a set of 3 isotropic thick layers stacked along the z-axis, for what the theory predicts to have a global transversely isotropic behaviour [5]. The cuboid's dimensions are L_x, L_y and L_z, and its faces' respective areas A_x (faces $x = 0$ and $x = 1$), A_y (faces $y = 0$ and $y = 1$) and A_z (faces $z = 0$ and $z = 1$).

The first simulation is a pure tension along the x-axis and is shown in Figure 1: static displacements are enforced along $+x$ and $-x$ to the nodes of the respective faces $x = 1$ and $x = 0$, with constraints of plane contact applied to the faces $y = 0$ and $z = 0$.

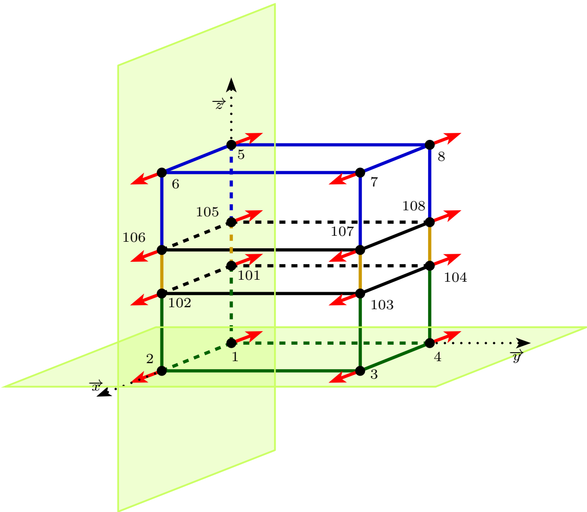

Figure 1: Pure tension along x

Computing the stress along direction x therefore leads to the Young's modulus E_x. For the other two Young's moduli, similar simulations can be applied in the directions y and z. The three Poisson's coefficients ν_{ij} can be computed with the displacements on the faces $y = 1$ and $z = 1$, with the aid of the general relation [20]:

$$\nu_{ij} = \frac{-\varepsilon_{jj}}{\varepsilon_{ii}} . \tag{2}$$

Finally, the equivalent material's shear moduli are computed by simulations of shear. Yet in the cases of anisotropic materials, and particularly for laminated composites, some attention must be paid for defining shear. Although the moduli are often defined without respect for either sliding or transverse shear configurations ([6, 20, 2, 1]), it may be observed in practice that the two behaviours are not equivalent in general. This is why in this paper, the analysis separates sliding shear (illustrated on Figure 2a) from transverse shear (illustrated on Figure 2b) in the respective "**O1**" and "**O2**" methods, which are yet completely equivalent for the determination of Young's moduli and Poisson's coefficients.

Sliding shear scheme $z - y$, which therefore corresponds to the "**O1**" method (see Figure 2a), combines an enforced displacement δ_y along $-y$ on face $z = 0$, the same displacement δ_y along $+y$ on face $z = 1$, and constraints of plane contact on the same faces $z = 0$ and $z = 1$ in order to generate pure shear. To stabilise the system, the degree of freedom Tx of node 1 is fixed. Computing the stress σ_{zy} yields the shear modulus G_{zy}. Finally, the two other shear moduli are then computed in a similar way, and the nine coefficients identified therefore define an equivalent orthotropic material entirely.

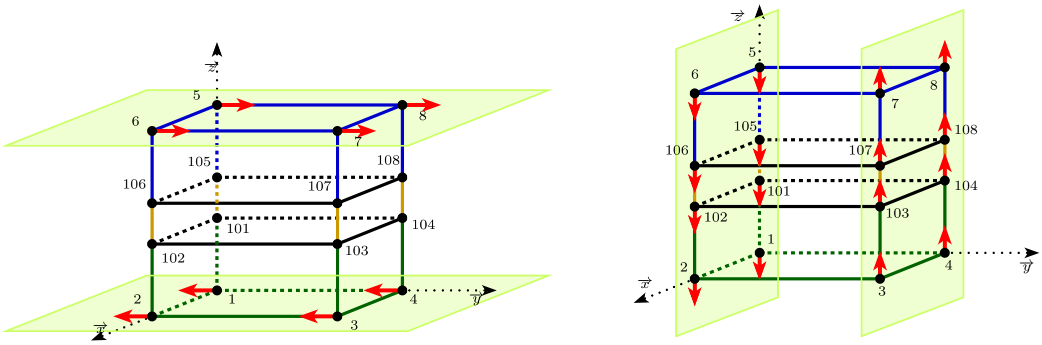

(a) Pure sliding shear $z - y$ (**O1**) (b) Pure transverse shear $y - z$ (**O2**)

Figure 2: Pure shear schemes

3 Experimental-numerical application on stators of electric machines

3.1 Identification of equivalent materials

Numerical and experimental projects involving laminated materials are numerous. During the last decade, electrical powertrains for hybrid and 100%-electric vehicles have come under the spotlight in the automotive industry [21]. More precisely, modelling the stator of an electric motor, generally consisting of a laminated steel stack, presents new challenges for predicting its mechanical behaviour. From a macroscopic view, the stack may consist in several hundreds of steel sheets whose thicknesses are about some tenths of millimetres. In this section, two different examples of finite element models of stators of electric motors are considered. The first model (called "**M1**") is shown on Figure 3, is made of 19,158 elements and 24,768 nodes for 12 teeth. The sheets are stacked along the z-axis, and different zones are detailed, each corresponding to a specific behaviour and therefore a specific material.

The first zone to be analysed is "*prox*", gathering the elements which are closest to the weld beads. In this zone, the proximity to the weld beads ensures the stator's tightest cohesion between the steel sheets, and imply therefore the best regularity in the successive varnish layers' thicknesses. This means that the cell <half-thick steel sheet; varnish sheet; half-thick steel sheet> is repeated regularly through the stator's length (dimension along z), with the same thicknesses everywhere. The industrial stator corresponding to the model on Figure 3, has been analysed experimentally. A modal basis has been measured on this structure, and stands for a reference in this section. The stator is composed of isotropic steel sheets of thickness 360 µm, separated by 3-µm-thick isotropic epoxy layers. The cell corresponding to the zone "*prox*" is thus a 3-layered cuboid with a square base of length 400 µm, and is detailed in Figure 4. In the FE model, the same density ρ is applied to all the zones, and directly

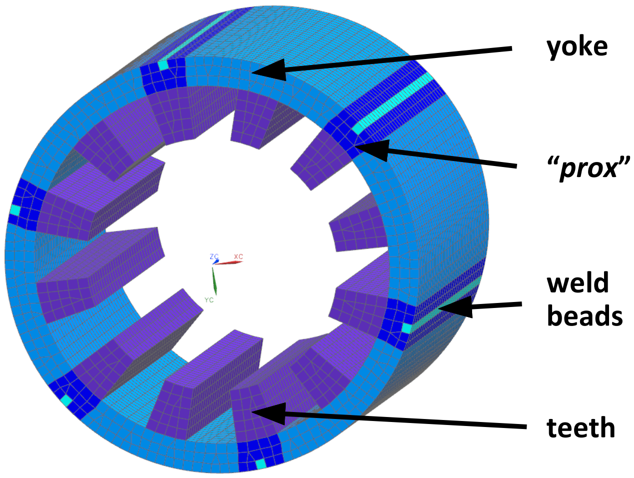

Figure 3: Zoning of the finite element model - stator "**M1**"

taken from the measurements on the stator:

$$\rho = \frac{m^{\text{tot}}}{V^{\text{tot}}} = 7750\,\text{kg}\cdot\text{m}^{-3}\ ,$$

where m^{tot} and V^{tot} respectively refer to the stator's total mass and volume.

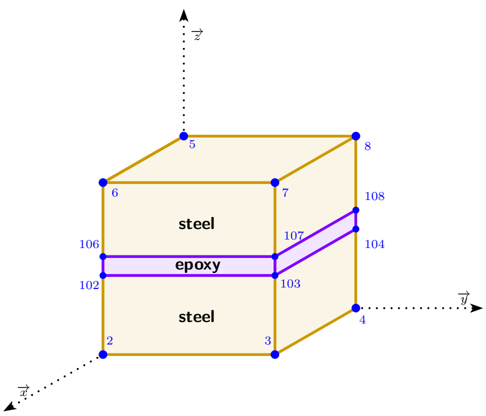

	Steel	Epoxy	Steel
E [GPa]	207	3.0	207
ν [$-$]	0.25	0.37	0.25
e [µm]	180	3	180

Figure 4: Base cell

Applying the method "**O1**" to the base cell of zone "*prox*" yields an equivalent material defined by the following elastic constants:

$$E_x^{\text{prox}} = E_y^{\text{prox}} = 205\,\text{GPa}\ , \qquad E_z^{\text{prox}} = 157\,\text{GPa}\ ,$$

$$G_{zy}^{\text{prox}} = G_{zx}^{\text{prox}} = 51.2\,\text{GPa}\ , \qquad G_{xy}^{\text{prox}} = 82.1\,\text{GPa}$$

and

$$\nu_{yz}^{\text{prox}} = \nu_{xz}^{\text{prox}} = \nu_{xy}^{\text{prox}} = 0.25\,.$$

Concerning the other zones, the factors 3/4 and 1/2 have been applied to the shear moduli of the respective zones "yoke" and "teeth", according to the distance to the weld beads. The other coefficients remain unchanged. Finally, the different material properties are detailed in Table 1. A picture of the experimental setting is shown on Figure 5.

	prox	**yoke**	**teeth**	**weld beads**
E_x [GPa]	205	205	205	207
E_y [GPa]	205	205	205	
E_z [GPa]	157	157	157	
G_{zy} [GPa]	51.2	38.4	25.6	-
G_{zx} [GPa]	51.2	38.4	25.6	
G_{xy} [GPa]	82.1	61.6	41.1	
ν_{yz} $[-]$	0.25	0.25	0.25	0.288
ν_{xz} $[-]$	0.25	0.25	0.25	
ν_{xy} $[-]$	0.25	0.25	0.25	
ρ $[\mathrm{kg} \cdot \mathrm{m}^{-3}]$	7750	7750	7750	7750

Table 1: Comparison of elastic coefficients - stator "**M1**"

3.2 Modal correlation

A convenient way of evaluating the similarities in the modal behaviours of two structures, a process of correlation can be computed. This aims at comparing the natural frequencies and the deformed shapes of the models by computing the matrices $[\Delta f]$ and $[MAC]$. Each component $\Delta f\,(m_{e,i}, m_{a,j})$ of the matrix $[\Delta f]$ expresses the relative difference between the natural frequency of the first structure's i-th mode $m_{1,i}$ and the second structure's j-th mode $m_{2,j}$, and is defined by the relation:

$$\Delta f\,(m_{1,i}, m_{2,j}) = \frac{f_{1,i} - f_{2,j}}{f_{1,i}}\ , \tag{3}$$

where $f_{1,i}$ et $f_{2,j}$ are the natural frequencies respectively corresponding to the modes $m_{1,i}$ and $m_{2,j}$. The second matrix, $[MAC]$, expresses the similarities between the deformed shapes of the modes $m_{1,i}$ and $m_{2,j}$ (respectively called $\{\phi_{1,i}\}$ and $\{\phi_{2,j}\}$), according to the so-called MAC criterion (*Modal Assurance Criterion*). Its components $MAC\,(m_{1,i}, m_{2,j})$ are defined by the expression [22]:

$$MAC\,(m_{1,i}, m_{2,j}) = \frac{\left|\{\phi_{1,i}\}^{\mathsf{T}}\{\phi_{2,j}\}\right|^2}{\{\phi_{1,i}\}^{\mathsf{T}}\{\phi_{1,i}\}\{\phi_{2,j}\}^{\mathsf{T}}\{\phi_{2,j}\}}\ . \tag{4}$$

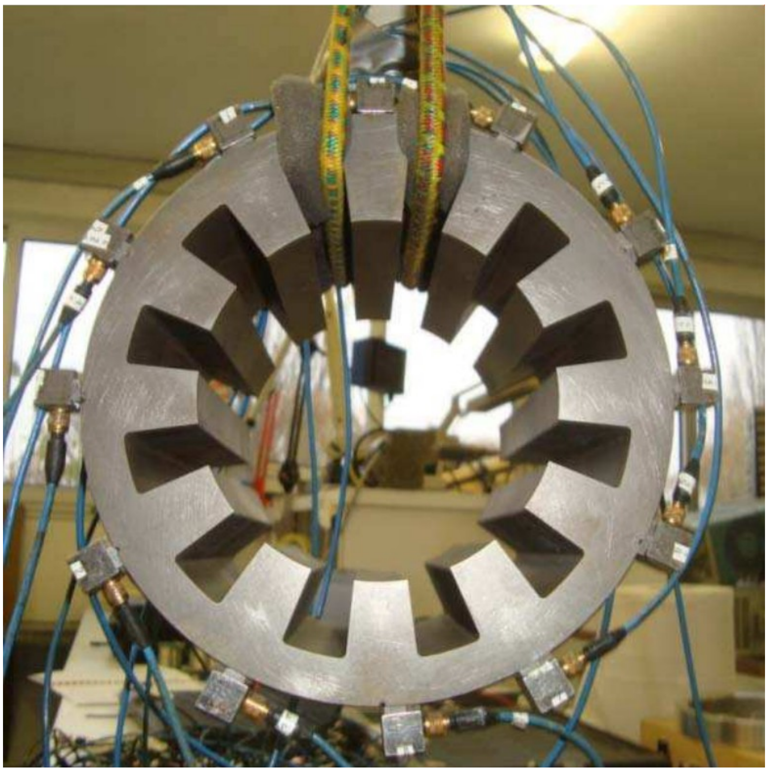

Figure 5: Experimental setting - stator "**M1**"

With these notions, two models perfectly correlated are defined by a matrix $[\Delta f]$ in which every diagonal component is at 0%, and a matrix $[MAC]$ in which every diagonal is at 100%, and the others at 0%. Finally, the pairs of modes for which MAC values are highest are assembled, and are taken into account for the correlation if the MAC values are above a fixed threshold.

3.3 Results

With the aid of the notions introduced in the previous paragraph, the correlation between the modal basis calculated from stator **M1**'s finite element model and the corresponding experimental data is computed. In addition to this, a correlation between simulation and measurements has been established for another stator: model **M2**, 48 teeth, 122,880 elements and 149,184 nodes. Considering similar production processes, identical materials have been used and applied in the same way for building model **M2**, with a similar zoning as for model **M1**. The results are described in Figure 6 and Table 2, where the columns "**FEA**" and "**EMA**" respectively refer to the mode frequencies in the FE model and in the experimental modal basis. The averages $\overline{|\Delta f|}$ and $\overline{MAC}$ have been computed in the bottom lines of Table 2. For both cases, only mode pairs for which MAC values were over 60% were taken into account.

Judging from these results, it can be observed that the materials computed with the

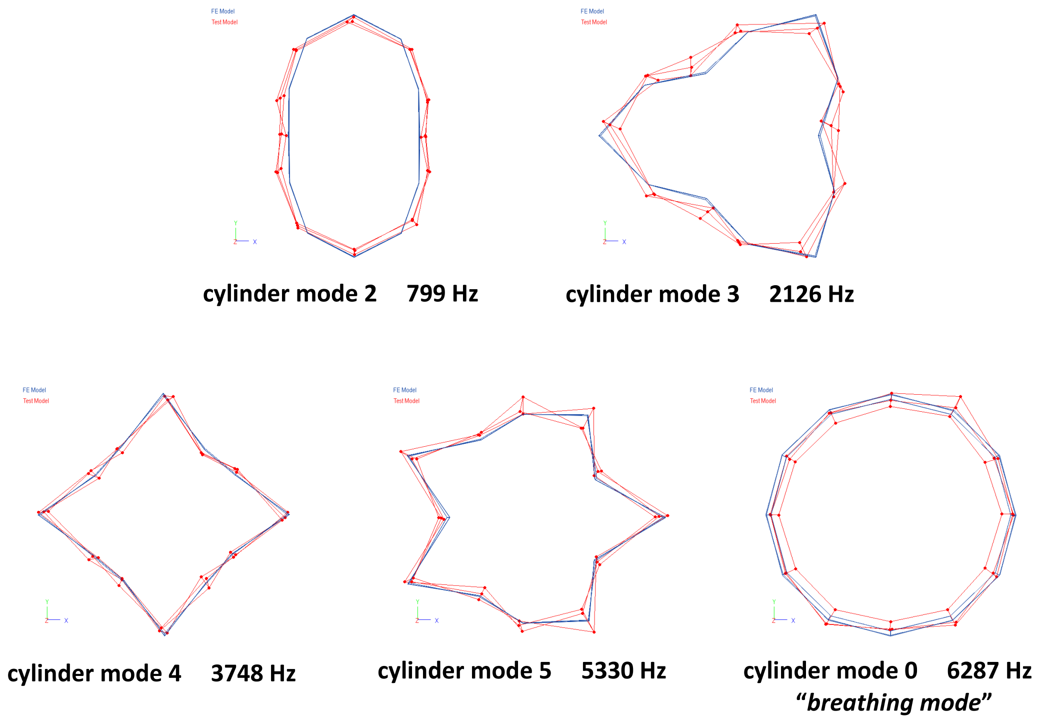

Figure 6: Correlation of FE and experimental modal bases - mode shape pairs (experimental frequencies for stator "**M1**") - blue lines: simulation, red dots: measurement

method "**O1**" are in good accordance with the measured natural frequencies, and are able to simulate the stators' first cylinder modes, which are most critical for acoustic considerations [23]. Model **M1**'s deformed shapes correspond to the experimental ones fairly well, and the fact that model **M2**'s MAC values are lower than **M1**'s can be explained by poorer quality in the corresponding experimental data, although the cylinder modes were easily spotted amongst all deformed shapes. Also, no model updating procedures on models **M1** and **M2** were able to increase their respective MAC values.

The results of Table 2 are compared with the case "**NZ**" (no zoning: the same "***prox***" material applied to the whole structure), as shown in Table 3.

It can be seen that the equivalent materials generated by method "**O1**" enable simulating the dynamic behaviours of entire structures accurately. In the cases of the real stators, the necessity of zoning the models and adapting the shear coefficients according to the elements' distances to the weld beads is shown as well. In comparison to the delicate measurements and time-consuming model-updating processes which are nowadays essential for simulating the dynamic behaviour of an electric machine's stator [21], using this simple and accurate way of computing equivalent materials for a representative equivalent FE model presents a new opportunity in the prediction and the design of such structures.

Mode pair	**FEA** [Hz]	**EMA** [Hz]	Δf [%]	MAC [%]	**Mode description**
M1 - 1	827.43	798.67	3.60	64.4	cylinder mode, order 2
M1 - 2	2148.9	2125.5	1.10	62	cylinder mode, order 3
M1 - 3	3814.5	3747.7	1.78	90.2	cylinder mode, order 4
M1 - 4	5397.2	5330.1	1.26	83.8	cylinder mode, order 5
M1 - 5	6199.6	6286.5	-1.38	77	cylinder mode, order 0
M1: *Averages* $\overline{\lvert\Delta f\rvert}$ ***and*** $\overline{MAC}$			***1.82***	***75.4***	
M2 - 1	1085.7	1060.1	2.41	69.7	cylinder mode, order 2
M2 - 2	2796.0	2782.6	0.48	45.4	cylinder mode, order 3
M2 - 3	4720.6	4713.5	0.15	21.4	cylinder mode, order 4
M2 - 4	5708.3	6050.5	-5.66	26.5	cylinder mode, order 0
M2: *Averages* $\overline{\lvert\Delta f\rvert}$ ***and*** $\overline{MAC}$			***2.17***	***40.8***	

Table 2: Correlations of FE and experimental modal basis - stators "**M1**" and "**M2**"

4 Conclusion

In this paper, a novel method for identifying equivalent materials to laminated orthotropic structures was proposed. Used in two experimental-numerical applications on stators of real electric motors, the method was proven able to simulate the first cylinder modes, which are of particular acoustic interest. In addition to this, the new methods can be applied to superelements too, unlike other existing homogenization techniques. Eventually, it is hoped that such methods will help improving the current knowledge about the behaviour of laminated structures, and in particular of stators of electric machines. Substituting time-consuming model updating procedures by a simple, direct method could even replace the manufacture of costly prototypes and the associated measurements.

References

[1] L. Gornet, *Généralités sur les matériaux composites*, 2008.

	M1		M2	
	Ortho1	NZ	Ortho1	NZ
$\overline{\lvert\Delta f\rvert}$ [%]	1.82	6.25	2.17	3.54
$\overline{MAC}$ [%]	75.4	75.0	40.8	40.8

Table 3: Influence of zoning

[2] J.M. Berthelot, *Composite materials, mechanical behavior and structural analysis*, Springer, 1999.

[3] J.N. Reddy, *Mechanics of Laminated Composite Plates and Shells, Theory and Analysis, 2nd Edition*, CRC Press, 2004.

[4] D. Begis, G. Duvaut, A. Hassim, "Homogénéisation par éléments finis des modules de comportements élastiques de matériaux composites", Technical Report 101, Institut National de Recherche en Informatique et Automatique, 1981.

[5] Y. Chevalier, J.V. Tuong, *Mechanics of viscoelastic materials and wave dispersion*, Iste/Wiley, 2010.

[6] D. Begis, A. Bestagno, G. Duvaut, A. Hassim, M. Nuc, "A new method of computing global elastic moduli for composite materials", Technical Report 195, Institut National de Recherche en Informatique et Automatique, 1983.

[7] A. Puck, "Grundlagen der Spannungs und Verformungs Analyse", *Dipl. Ing. Kunststoffe, Bd*, 57(4), 1967.

[8] S.W. Tsai, J.C. Halpin, N.J. Pagano, R.T. Schwartz, *Composite materials workshop*, Technomic, 1968.

[9] D. Lukkassen, L.E. Persson, P. Wall, "Some engineering and mathematical aspects on the homogenization method", *Composites Engineering*, 5(5): 519–531, 1995.

[10] P.W. Chung, K.K. Tamma, R.R. Namburu, "Asymptotic expansion homogenization for heterogeneous media - computational issues and applications", *Composites Part A - Applied Science and Manufacturing*, 32(9): 1291–1301, 2001.

[11] E.M. Hassan, A.V. Georgiades, M.A. Savi, A.L. Kalamkarov, "Analytical and numerical analysis of 3D grid-reinforced orthotropic composite structures", *International Journal of Engineering Science*, 49(7): 589–605, 2011.

[12] A.L. Kalamkarov, E.M. Hassan, A.V. Georgiades, M.A. Savi, "Asymptotic homogenization model for 3D grid-reinforced composite structures with generally orthotropic reinforcements", *Composite structures*, 89(2): 186–196, 2009.

[13] R.F.S. Hearmon, "The elastic constants of anisotropic materials", *Reviews of Modern Physics*, 18(3): 409, 1946.

[14] M. Hayes, "A simple statical approach to the measurement of the elastic constants in anisotropic media", *Journal of Materials Science*, 4(1): 10–14, 1969.

[15] F. Pierron, S. Zhavoronok, M. Grédiac, "Identification of the through-thickness properties of thick laminated tubes using the virtual fields method", *International Journal of Solids and Structures*, 37(32): 4437–4453, 2000.

[16] R. Rikards, A. Chate, W. Steinchen, A. Kessler, A.K. Bledzki, "Method for identification of elastic properties of laminates based on experiment design", *Composites Part B: Engineering*, 30(3): 279–289, 1999.

[17] R. Rikards, A. Chate, G. Gailis, "Identification of elastic properties of laminates based on experiment design", *International Journal of Solids and Structures*, 38 (30): 5097–5115, 2001.

[18] R. Rikards, "Identification of mechanical properties of laminates", *Modern Trends in Composite Laminates Mechanics*, (448): 181, 2004.

[19] A.L. Araújo, M. Soares, M.J. Moreira de Freitas, P. Pedersen, J. Herskovits, "Combined numerical-experimental model for the identification of mechanical properties of laminated structures", *Composite Structures*, 50(4): 363–372, 2000.

[20] Y. Chevalier, *Comportements élastique et viscoélastique des composites*, Volume 5, Techniques de l'Ingénieur, 1988.

[21] J.B. Dupont, P. Bouvet, L. Humbert, "Vibroacoustic simulation of an electric motor: methodology and focus on the structural FEM representativity", in *International Conference on Electrical Machines*, pages 1–7. Marseille, September 2012.

[22] D.J. Nefske, S.H. Sung, "Correlation of a Coarse-Mesh Finite Element Model Using Structural System Identification and a Frequency Response Assurance Criterion", in *Proceedings of the International Modal Analysis Conference*, pages 597–602, 1996.

[23] J.B. Dupont, P. Bouvet, "Multiphysics Modelling to Simulate the Noise of an Automotive Electric Motor", *SAE International*, 2012.